Use of AIRSAR (POLSAR) data for quantifying the biomass of woodlands, Queensland, Australia.

R.M. Lucas[1], P. Tickle[2], A. Lee[3], J. Austin[3], C. Witte[4] , K. Jones[4], N. Cronin[5], M. Moghaddam[6] and A.K.Milne[5]

[1]Institute of Geography and Earth Sciences, The University of Wales, Aberystwyth, Aberystwyth, Ceredigion, SY23 3DB, United Kingdom (rml@aber.ac.uk); [2]Raytheon Australia, Imagery and Geospatial Systems, Brindabella Business Park, Canberra Airport, ACT 2609, Australia. [3]Bureau of Rural Sciences and Cooperative Research Centre for Greenhouse Accounting, PO Box E11, Kingston, ACT, 2604 Australia. [4]Forest Ecosystem Assessment and Planning, Queensland Department of Natural Resources, Resource Sciences Centre, 80 Meiers Road, Indooroopilly, Queensland, 4068, Australia. [5]School of Geography, The University of New South Wales, Kensington, NSW, 2052, Australia. [6]Jet Propulsion Laboratory, NASA, Pasadena, CA, USA.

ABSTRACT

To evaluate the potential of Synthetic Aperture Radar (SAR) for retrieving the Above Ground Biomass (AGB) of Australian woodlands, preliminary relationships were established between the biomass (scaled-up from field measurements using laser scanner) of different communities (distinguished using Large Scale Photography) and AIRSAR (POLSAR) data acquired over a 40 x 60 km woodland area near Injune, central Queensland, during PACRIM II. Preliminary analysis suggest that AGB could be retrieved using SAR, with L-band VV data being the most suitable if regression analyses are used.

INTRODUCTION

The research aimed to evaluate the potential of polarimetric Synthetic Aperture Radar (SAR) for quantifying the biomass and structural diversity of woodlands in Queensland, Australia. Information on biomass is required to support regional calculation of carbon budgets and, when combined with structural information, assist in the sustainable utilisation of forests and conservation of biodiversity. The PACRIM II mission presented an ideal opportunity to evaluate this potential (using AIRSAR) and to assess the potential of future spaceborne SAR (e.g., the Advanced Land Observing System (ALOS) Phased Array L-band SAR (PALSAR)) for regionally estimating woodland biomass and structure.

STUDY AREA

The study focused on a 40 x 60 km area of woodland near Injune, which is located in the Southern Brigalow Belt (SBB), a biogeographic region of southeast and central Queensland (Figure 1). More than 50 % of clearing in Queensland has occurred in the SBB and has been attributed largely to the establishment of cattle pasture, the expansion of the wheat farming and, more recently, the formation of cotton fields. Partial clearance of vegetation has also been commonplace in the pastoral areas and woody thickening is widespread. Some areas support commercial forestry activities. Due to the complex nature of land use and management practices, the landscape consists of a mosaic of cleared fields and forest and woodland communities in various stages of degradation and/or regeneration.

Within the Injune study area, the gently undulating country supports white cypress pine (*Callitris glaucophylla*) stands on the sandy hills. The more alluvial clays in the valleys are dominated by poplar box (*E. populnea*), silver-leaved ironbark (*E. melanaphloia*) and brigalow (*A. harpophylla*) communities.

EXPERIMENTAL DESIGN

A systematic grid of 150 (10 columns and 15 rows) of 150 x 500 m Primary Sampling Units (PSUs) was established across the 40 x 60 km study area. Each PSU centre was located 4 km apart in the north-south and east-west directions (Figure 1). All PSUs were divided into 30 Secondary Sampling Units (SSU), 50 x 50 m in dimension and numbered progressively by row from top left (1) to bottom right (30).

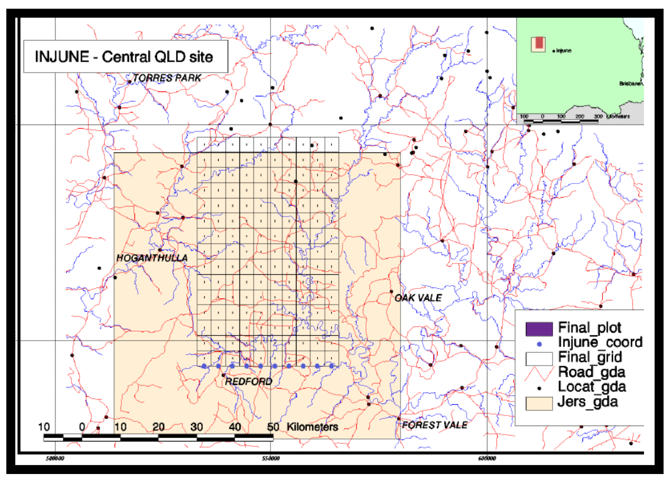

Figure 1: The Injune study area and sampling design

On July 14th, 2000, and prior to the field campaign, 1:4000 Large Scale colour stereo aerial Photographs (LSP) were acquired using a RC20 large format photographic camera. Global Positioning System (GPS) coordinates were recorded for each photo principal point to within a nominal precision of ± 20 m of the absolute location. The acquisition was planned such that the 50 ha stereo overlap for each photo pair was centred on the PSU area. Using the overlap area of each of the 150 stereo pairs, the main vegetation types were identified and delineated manually by a trained photogrammetrist and described in terms of their species composition, height, cover and disturbance (Jones et al., 2000). Using this information, PSUs representing the main vegetation types and regeneration stages at Injune were identified. From these, the PSUs assigned for subsequent field survey were selected, with the final selection based on accessibility.

In August, 2000, lidar data (Optech 1020 scanner mounted in a Bell Jet Ranger helicopter; 1 m spatial resolution, footprint of 25 cm) and hyperspectral data (Compact Airborne Spectrographic Imager (CASI), 1 m spatial resolution, 14 wavebands) were acquired for each of the 150 PSUs. The Optech 1020 lidar operates within the NIR spectrum and measures 500 first and last returns and also the intensity of each return per second. Lidar data were acquired at a nominal altitude of 250 m and a swath width of approximately 200m, a flight configuration that ensured lidar coverage of each PSU and resulted in a lidar footprint of < 15 cm and average sampling interval of < 1 m. A GPS base station was established during both lidar and CASI flights to ensure accurate georeferencing of the data.

At the same time as the laser and CASI overflights, field data were collected from 36 50 x 50 m SSUs located within 12 of the 150 PSUs such that the main vegetation types and regeneration stages were represented. For each SSU, field data collected included the locations of all trees > 5 cm diameter (at 130 cm) and their diameter (at 30 and 130 cm), height, crown dimensions and growth stage. Each tree was identified to species. Digital photographs were taken of at least every 10^{th} tree and Foliage Projected Cover (FPC) was measured at 1 m intervals along three 50 m transect lines. Following field data collection, destructive harvesting of the major tree species (*Callitris glaucophylla*, *Eucalpytus crebra*, *Eucalpytus populnea*, *Acacia harpophylla*) across the diameter range was undertaken to facilitate estimation of the above ground and, in the case of *C. glaucophylla*, below ground biomass components. The above ground biomass (AGB) components included leaves and both branches and trunks divided into discrete size classes (e.g., 1-4 cm, 4-10 cm, 10-20 cm).

On the 3^{rd} September, 2000, the NASA JPL DC-10 acquired four strips (10 x 80 km) of polarimetric SAR (POLSAR) data across the entire PSU grid. One strip of topographic SAR (TOPSAR) and four strips of hyperspectral MASTER (TERRA-1 MODIS ASTER simulator) data were also acquired over the 40 x 60 km study area. Landsat ETM+ data and ASTER data were also acquired over the same time period.

PROCESSING STAGES

This section focuses solely on the processing of LSP, lidar and POLSAR data and the subsequent integration of these data.

LSP

Photoprints of the LSP were scanned to 600 dpi and then enlarged to 1:1000 scale to facilitate individual tree mapping. Initial rectification was undertaken using the known locations of principal points and camera parameters. Comparisons with the lidar and other datasets confirmed that rectified LSP were generally accurate to within ± 20 m without additional registration. The spatial accuracy of the LSP was, however, refined further by establishing common Ground Control Points (GCPs) with the lidar data and performing a polynomial transformation. Root Mean Square (RMS) errors of < 2 m were obtained. The polygon linework used initially to delineate the vegetation communities within each PSU was then scanned, vectorised and rectified using the same transformation as the digital imagery.

Lidar

An accurate bare earth Digital Elevation Model (DEM) was generated for each PSU from the lidar data by extracting the lowest lidar returns within 10 x 10 m windows, from which a Triangular Irregular Network (TIN) was generated. The resultant TIN was then checked visually to confirm correct classification of ground returns and transformed into a 1 m grid using bilinear interpolation methods. The height of each lidar vegetation return was then calculated as the difference between the elevation of the ground DEM and the elevation of the vegetation return.

The lidar data were then sliced horizontally to produce foliage cover surfaces at 5 m height intervals (which relates to the vertical distribution of foliage). The 5-m intervals were chosen as a compromise between minimising the number of explanatory variables in the subsequent step-wise regression, adequately describing the significant structural variability up to 35 m, and including (in some cases) a small number of large, tall trees which would have significant impact on biomass at the plot level. A step-wise linear regression was then undertaken using the multiple input surfaces against the plot-based estimates of biomass. The relationship between the estimates of biomass generated for each SSU and the proportion of lidar returns within each height class is shown in Equation 1.

$$Y = \_{}_1\_{}_1 + \_{}_2\_{}_2 + \cdots + \_{}_6\_{}_6 + \_ \qquad \text{Equation (1)}$$

Where Y = ABG (Mg ha^{-1}) and $\_{}_n$ and $\_{}_n$ represent the proportion of lidar vegetation hits for given height classes and the corresponding regression coefficients respectively (Table 1).

Table 1: Height classes for _n variables (proportion of lidar vegetation hits within height class (m)) and the regression coefficients (_n) for each height class.

Variable number	Proportion of lidar vegetation hits within height class (m; _)	Regression coefficient for height class (_)
1	0.5-5.0	0.168
2	5.0-10.0	1.947
3	10.0-15.0	0.857
4	15.0-20.0	3.589
5	20.0-25.0	19.910
6	25.0-35.0	20.00

The lidar predictions generated a strong linear relationship with an adjusted r^2 of 0.89 and SE of 11.01 Mg ha^{-1}. As the ground estimates of biomass were not free of error, the lidar predictions were plotted back over the field estimates, revealing that 69 % fell within the 95 % confidence limits of the data. A t-test of the two estimates also revealed no significant difference ($P < 0.05$) between the lidar and field-based predictions of biomass. A 0.25 hectare spatial resolution estimate of biomass, as predicted using Equation 1 is shown in Figure 2. Fully automated procedures were then applied across all 150 PSUs, thereby generating 4,500 estimates of total biomass.

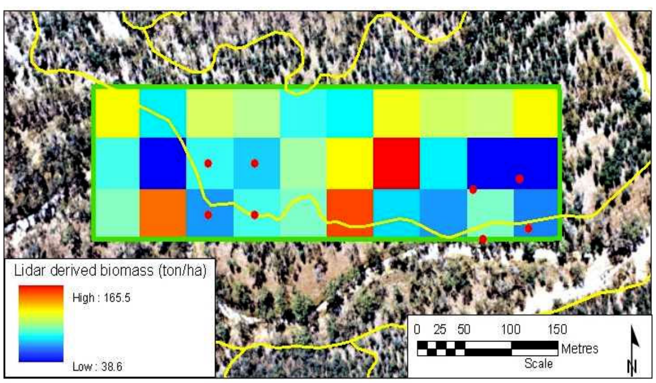

Figure 2: Predictions of total AGB (as generated using Equation 1) for each of 30 SSU within 1 PSU (with the backdrop of the stereo aerial photograph.

POLSAR data

The four strips of POLSAR data , consisting of three fully polarimetric frequencies (C-, L-, and P-bands) for a total of 12 bands per strip, were provided in 16-look Stokes matrix format with a pixel spacing of 4.62 m in range and 4.62 m in azimuth. The incidence angle ranged from 20^o to 60^o. The POLSAR data were synthesized (to intensity values) within IDL ENVI and slant-to-ground range corrected (nominal resolution of 4.62 m). Geometric correction was performed by establishing common GCPs between the POLSAR data and a Landsat ETM+ image of the Injune study area, acquired in September, 2000. This image was rectified, to a high level of precision, by the Queensland Department of Natural Resources (QDNR) Statewide Landcover And Trees Study (SLATS) project to Universal Transverse Mercator (UTM) coordinates. Between 100-150 GCPs were established for each POLSAR strip, generating RMS errors of <10 m. Geometric correction was achieved using a 3rd order nearest neighbour polynomial transformation. The POLSAR strips were then combined to produce a seamless mosaic for the Injune area (Figure 3).

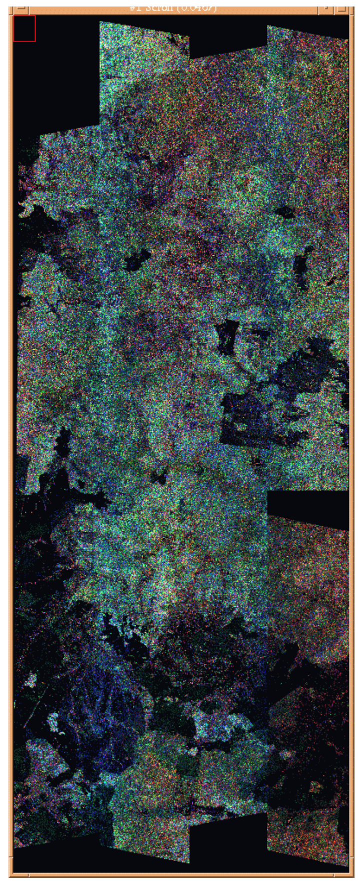

Figure 3: POLSAR mosaic of the Injune study area

Data integration

An ArcInfo coverage representing each of the 4500 SSUs within the Injune study area was overlain onto the POLSAR mosaic. The corresponding POLSAR backscatter values (L and P band, co- and cross-polarisations) were then extracted for each SSU and related, by community (determined using LSP), to the AGB, as estimated using the lidar data. C-band data were not extracted, as the data required further processing at JPL. In this paper only data associated with 750 of the 4500 SSUs (~ _ POLSAR strip) are presented.

RELATIONSHIPS WITH AGB

Preliminary observations suggest that at both L and P-band (all polarisations), there is a strong relationship with AGB. Figures 4 and 5 give examples of this relationship, as observed using L-band HV and L-band VV. In the POLSAR image selected, there were few woodlands with a biomass of less than 50 Mg ha^{-1}. For this reason, the relationship with SAR backscatter can only be inferred for this biomass range. However, the results suggest that the strength of the relationship is greater in the lower biomass range but weakens in the higher biomass woodlands due to a diversification of structures and sizes of the woody components. Even so, the scatter in the relationship is indicative of the different structural types.

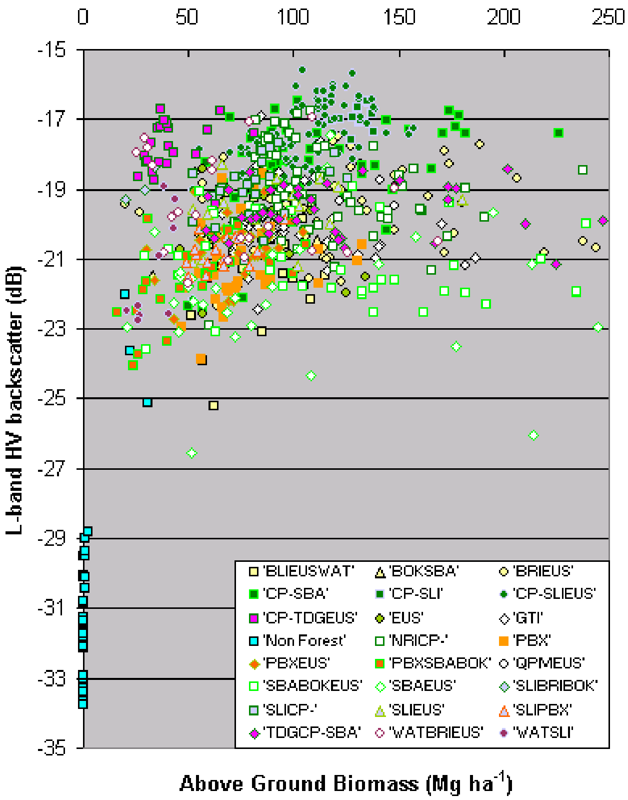

Figure 4: Relationship between L-band HV backscatter and above ground biomass, as estimated for 750 PSU by using lidar data as input to Equation 1. The codes are as follows: BLI: *E. fibrosa* ssp. *Nubila* (Blue-leaved Ironbark); BOK: *Allocasuarina luehmannii* (Bull Oak); BRI: *E. fibrosa* ssp. *Fibrosa* (Broad-leaved Red Ironbark); CP- *C. glaucophylla* (Cypress Pine); EUS: *Eucalyptus* sp. NRI: *E. crebra* (Narrow-leaved Ironbark); PBX: *E. populnea* (Poplar Box) QPM: *E. exserta* (Queensland peppermint) SBA; *A. leiocarpa* (Smooth Barked Apple); SLI: *E. melanaphloia* (Silver-leaved Ironbark); TDG: *E. dealbata* (Tumbledown Gum); WAT: *Acacia* sp. The first code represents the most dominant species.

The analysis suggests that, for a regression-type analysis, L-band VV data are perhaps better suited than L-HV for quantifying woodland biomass as structural differences between community types are less exaggerated, although the dynamic range of the data is reduced compared to L-band HV.

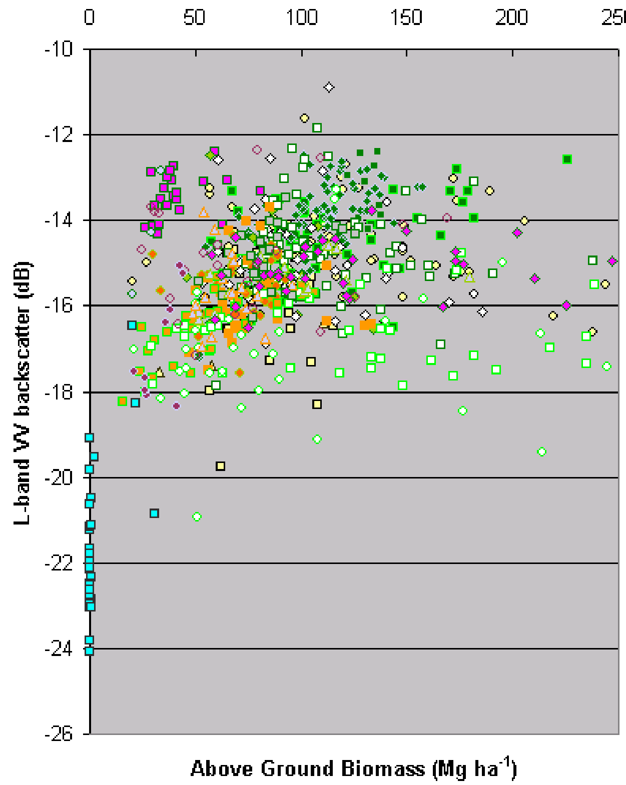

Figure 5: Relationship between L-band VV backscatter and AGB. Refer to Figure 5 for the marker legend.

The main scatter within both relationships can be attributed to woodlands that are dominated by or include *A. leiocarpa* (**SBA**BOKEUS, **SBA**EUS, TDGCP-**SBA**, CP-**SBA**). This species is dispersed throughout the woodlands at Injune and is unique in that mature individuals are typically much larger than other woodland species, support expansive crowns and allocate much of their biomass to branches (Figure 6).

a)

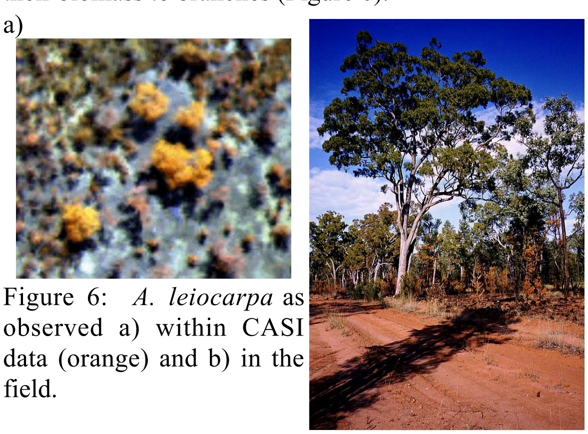

Figure 6: *A. leiocarpa* as observed a) within CASI data (orange) and b) in the field.

An unusual distribution in the relationships is also observed for woodlands co-dominated by *C. glaucophylla* and *E. dealbata* (Tumbledown Gum; CP-TDGEUS).

When only woodlands dominated by *C. glaucophylla*, *E. melanaphloia* and *E. populnea* are considered, the use of L-band VV data alone seems viable for retrieving AGB. Although further investigation is required, prior classification of woodland types using, for example, Landsat ETM+, MASTER or ASTER data (acquired in 2000) or Hyperion data (acquired over Injune in 2002), and subsequent integration of SAR data for estimating the biomass of the mapped communities may increase the accuracy of AGB retrieval using regression analyses.

MODELLING SAR BACKSCATTER

The research confirms the potential of SAR data for retrieving the AGB of woodlands. However, to improve the retrieval of AGB, knowledge of how microwaves interact with different structural and biomass components (i.e., leaves, branches, trunks) of woodlands is necessary. An approach is to establish regression relationships between the biomass of these components and the SAR backscatter at different wavelengths and polarisations. This analysis is ongoing and is the subject of forthcoming papers. An alternative approach is to simulate microwave interaction with the woodlands based on knowledge of the vertical and horizontal distribution of scatterers (as determined from field measurement) and their moisture content, which together determine the component biomass values.

A preliminary investigation into SAR backscatter simulation has therefore been undertaken by considering two woodland communities dominated by the species *C. glaucophylla* (Figure 7) and *E. populnea* (Figure 8) respectively.

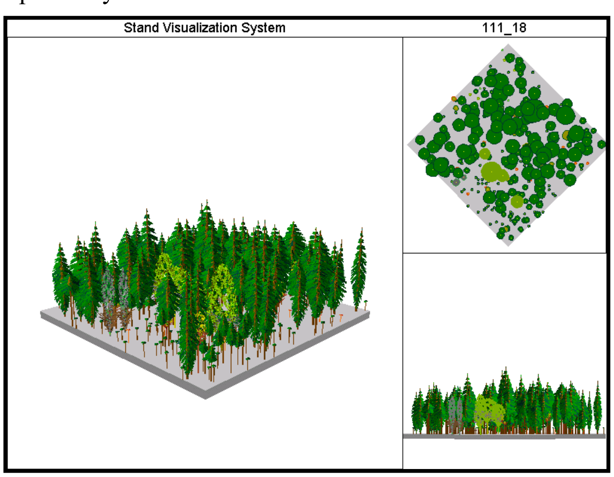

Figure 8: Three-dimensional visualisation of *C. glaucophylla*-dominated woodland.

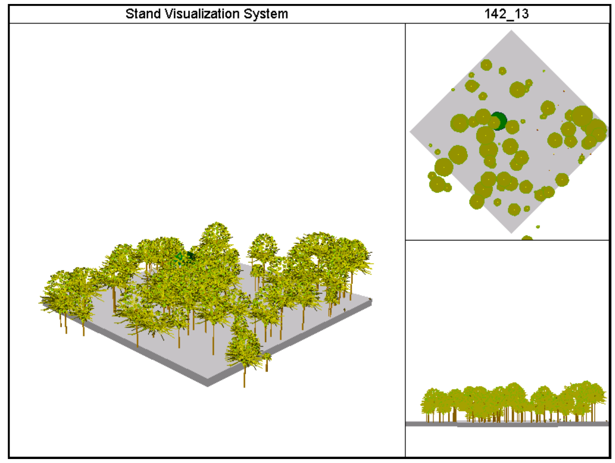

Figure 9: Three-dimensional visualisation of *E. populnea*-dominated woodland.

The woodlands differ in that the *C.glaucophylla* supports a greater biomass (Figure 4), with most allocated to the trunk. The trunks are typically vertical in their orientation and tree density is relatively high (e.g., 600 trees ha^{-1}). In contrast, *E. populnea* supports a lower biomass, with approximately 40% allocated to the branches. The branches are angled at 30 ^{o} to 40^{o} from vertical and tree density is lower (e.g., 300 trees ha^{-1}).

For each SAR frequency and polarization, an existing numerical discrete-component forest scattering model developed at JPL is used to simulate the theoretical radar backscatter values as functions of various stand geometrical and moisture variables. To reduce the number of free variables, allometric relations for each species type can be used to express various canopy parameters in terms of others. By carrying out the simulations at many values within physically acceptable ranges of each parameter (or technically, variable), parametric families of curves are generated. Higher-order multlidimensional polynomials are then fit into these curves, producing closed-form representations of the complex numerical scattering process. Estimates of free variables are then obtained through an algorithm that produces the optimal variable resulting in the best match between SAR measurements and the closed form polynomial model.

The above technique is applied first at higher frequencies (C- and L-bands) to estimate the variables describing the top layers of the forest canopy (branch-layer component geometry and moisture). With the top layers characterized, their contribution to SAR backscatter at lower-frequencies (P- and L-band a appropriate) is simulated numerically and subtracted from the total backscatter at those frequencies. The remaining backscatter values then contain information about the lower layers of vegetation only, and can be similarly used to estimate the variables contained in those layers (such as trunk diameter and moisture content, and soil moisture). Note that this technique enables the characterization of up to two vegetation layers. Preliminary results will be shown at the presentation. If more vertical segmentation is needed, further model development and/or more data types, such as interferometric SAR, may be needed. This approach can also be extended to include optical data in addition to the SAR backscatter data through appropriate optical modeling.

DISCUSSION AND CONCLUSIONS

Although preliminary, the research confirms the potential of polarimetric SAR for retrieving the AGB of woodlands in Australia, as suggested previously by Lucas *et al.* (2000). The strength of the relationship is anticipated to be increased through a) correction for incidence angle effects, b) improved estimation of AGB and component biomass from both field data and through integration of CASI (for species discrimination and tree crown/cluster delineation) and laser for spatial extrapolation, c) better understanding of microwave interaction with different biomass and structural components through observation and modelling, d) inclusion of AGB data for woodlands < 50 Mg ha^{-1} and e) integration of optical/hyperspectral data (e.g., for estimating leaf biomass).

The study indicates that L-band VV data may be most suited for quantifying AGB through regression analyses, as backscatter is relatively independent of woodland structure. L-band HV data may, however, provide important information on the structure of forests. These observations suggest that the forthcoming ALOS PALSAR, which will routinely provide L-band polarimetric data, may be well suited to quantifying the AGB of woodlands in Queensland and in other regions of Australia. Even so, prior classifications of woodland types generated using optical/hyperspectral data, may be important in refining the estimates of biomass. Although these types of simplified regression-based retrievals are important in obtaining a rough estimate of biomass values, more accurate and reliable estimates are obtained only through more analytical techniques that relate SAR backscatter to fundamental scattering properties of forest stands from which component biomass values can be calculated.

ACKNOWLEDGMENTS

The authors would like to acknowledge the support provided by the Australian Research Council (ARC) under their SPIRT program, staff of the UNSW, QDNR, BRS, QUT, QDPI TBC, the CRC Carbon Accounting, the Australian Greenhouse Office, Agriculture Fisheries and Forestry, and QDPI TBC. Gunn Resources, BALL AIMS and NASA are thanked for their assistance in acquiring the laser, CASI and POLSAR data respectively.

REFERENCES

Jones, K.L. 2000. Aerial photography interpretation for the Injune remote sensing sampling strategy. Forest Ecosystem Research and Assessment Technical Report No. 00129. Queensland Department of Natural Resources, Brisbane, Australia.

Lucas, R.M., Milne, A.K., Cronin, N., Witte, C. and Denham, R. 2000. The potential of Synthetic Aperture Radar (SAR) for quantifying the biomass of Australia's woodlands. . *Rangeland Journal*, **22**, 124-140.